Earth, Planets and Space
a SpringerOpen Journal

LETTER Open Access

Friction properties of the plate boundary megathrust beneath the frontal wedge near the Japan Trench: an inference from topographic variation

Hiroaki Koge[1*], Toshiya Fujiwara[2], Shuichi Kodaira[2], Tomoyuki Sasaki[3], Jun Kameda[4], Yujin Kitamura[5], Mari Hamahashi[1], Rina Fukuchi[6], Asuka Yamaguchi[6], Yohei Hamada[2], Juichiro Ashi[6] and Gaku Kimura[1]

Abstract

The 2011 Tohoku-Oki earthquake (Mw 9.0) produced a fault rupture that extended to the toe of the Japan Trench. The deformation and frictional properties beneath the forearc are keys that can help to elucidate this unusual event. In the present study, to investigate the frictional properties of the shallow part of the plate boundary, we applied the critically tapered Coulomb wedge theory to the Japan Trench and obtained the effective coefficient of basal friction (μ_b') and Hubbert-Rubey pore fluid pressure ratio (λ) of the wedge beneath the lower slope. We extracted the surface slope angle and décollement dip angle (which are the necessary topographic parameters for applying the critical taper theory) from seismic reflection and refraction survey data at 12 sites in the frontal wedges of the Japan Trench. We found that the angle between the décollement and back-stop interface generally decreases toward the north. The measured taper angle and inferred effective friction coefficient were remarkably high at three locations. The southernmost area, which had the highest coefficient of basal friction, coincides with the area where the seamount is colliding offshore of Fukushima. The second area with a high effective coefficient of basal friction coincides with the maximum slip location during the 2011 Tohoku-Oki earthquake. The area of the 2011 earthquake rupture was topographically unique from other forearc regions in the Japan Trench. The strain energy accumulation near the trench axis may have proceeded because of the relatively high friction, and later this caused a large slip and collapse of the wedge. The location off Sanriku, where there are neither seamount collisions nor rupture propagation, also has a high coefficient of basal friction. The characteristics of the taper angle, effective coefficient of basal friction, and pore fluid pressure ratio along the Japan Trench presented herein may contribute to the understanding of the relationship between the geometry of the prism and the potential for generating seismo-tsunamigenic slips.

Keywords: Japan Trench; Topography; Critical taper; Tohoku-Oki earthquake; Basal friction; Surface slope angle; Seismo-tsunamigenic slip; Taper angle; Pore fluid pressure ratio; Prism

Correspondence/Findings

Introduction

The 2011 Tohoku-Oki earthquake (Mw 9.0) produced a fault rupture that extended to the shallow portion of the Japan Trench. Based on bathymetry changes from before to after the earthquake, Fujiwara et al. (2011) demonstrated that the seafloor of the outermost part of the landward trench slope moved approximately 50 m toward the trench and was uplifted by approximately 7 to 10 m. The large fault rupture and propagation might have been due to the essentially weak fault material and dynamic weakening (Ujiie et al. 2013) and/or abnormal fluid pressure along the megathrust (Kimura et al. 2012). Fujie et al. (2013) researched the along-trench variation of the structure with seismic surveys in the northern Japan Trench, and their data suggest that there is a good correlation between the seismic structure and segmentation of the interplate coupling. This implies that the

* Correspondence: h.kouge@eps.s.u-tokyo.ac.jp
[1]Department of Earth and Planetary Science, The University of Tokyo, Tokyo 113-0033, Japan
Full list of author information is available at the end of the article

variations in the forearc structure are closely related to those in the interplate coupling. The deformation and frictional properties (the effective coefficient of basal friction and pore fluid pressure ratio) beneath the forearc are the keys to elucidating this unusual event.

Kimura et al. (2012) focused on seismic reflection data along a seismic transect of the ruptured area at the Japan Trench, and they measured the taper angle and estimated the effective coefficient of basal friction at the plate boundary by using the critically tapered Coulomb wedge theory (Davis et al. 1983; Dahlen 1984). However, a limited profile from the narrow area is not enough to understand the frictional properties of the plate boundary in comprehensive areas of the Japan Trench. In the present study, we therefore used 12 profiles (Figure 1) to calculate the effective coefficient of basal friction at the plate boundary with the intent of better understanding the along-trench variation (e.g., Fagereng 2011). From these results, we discuss the relationship between the geometry of the prism and tsunamigenic slip in the Japan Trench.

Tectonic setting

The Japan Trench is located to the east of northeastern Japan, and its north and south limits are known to have fairly sharp changes in orientation. The Japan Trench at its northern perimeter is separated from the Kurile Trench by a ridge at southern Hokkaido toward the southeast (Figure 1), and at its southern perimeter, the trench is separated from the Izu-Bonin Trench by a ridge extending eastward from Cape Inubo in central Japan (Dietz 1954). The mean depth of the Japan Trench axis is approximately 7.58 km (calculated from Tsuru et al. 2002). According to the NUVEL-1A model (DeMets et al. 1994), the Pacific Plate is subducting beneath the Japanese islands at a rate of approximately 92 mm/year in a 292° direction toward the fixed Eurasian Plate. The subducting direction changed from NNW to SSE to WNW to ESE at approximately 46 Ma and has been constant since that time (von Huene and Lallemand 1990). The current age of the Pacific Plate along the Japan Trench is approximately 130 to 140 Ma, as defined by a geomagnetic anomaly (Nakanishi et al. 1989; Tominaga et al. 2008).

The Japan Trench is interpreted to be an erosive margin, where the tectonic erosion proceeds with the subduction of the Pacific Plate (von Huene and Lallemand 1990). Legs 56 and 57 of the Deep Sea Drilling Project (DSDP) survey revealed that the material constituting the landward slope has been eroded and the inboard trench slope has been subsiding since the Miocene (von Huene and Lallemand 1990). The seafloor topography of

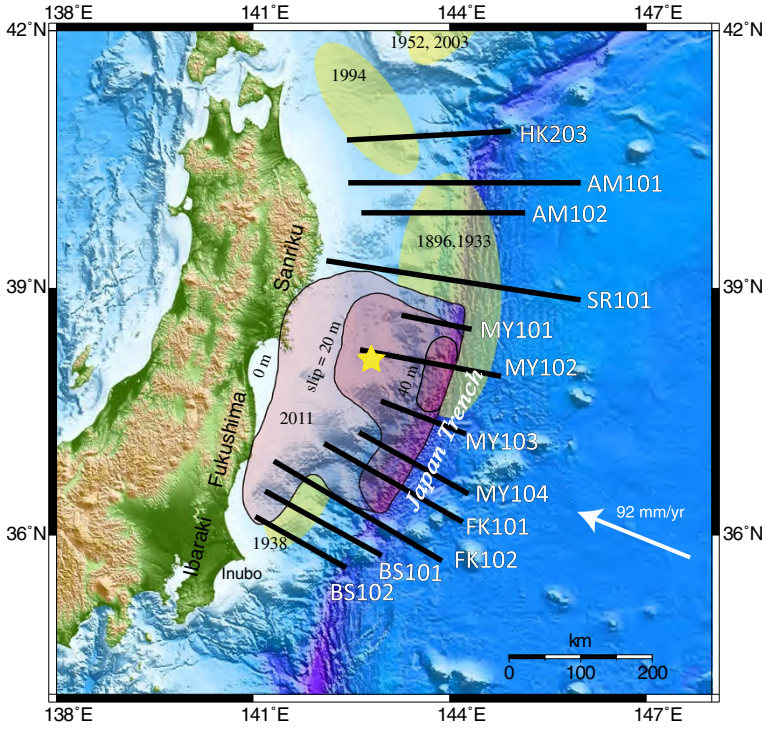

Figure 1 Location map of the Japan Trench and the index of 12 profiles from seismic surveys. Location map of the Japan Trench and the index of 12 profiles from seismic surveys across the trench axis before the 2011 Tohoku-Oki earthquake. The names of lines match the names of survey lines managed by JAMSTEC. The star represents the epicenter of the earthquake. The yellow ellipses represent the slip areas of past major earthquakes and the estimated ages are given (Tajima et al. 2013). A simple contour represents the slip area of the 2011 Tohoku-Oki earthquake (Chester et al. 2013).

the forearc off northeastern Japan is divided roughly into four parts: a deep-sea terrace and upper, middle, and lower slopes (Figure 2). The deep-sea terrace is defined as a deposition surface of the forearc basin with approximately 100-km EW width off Fukushima around survey sites FK101 and FK102 (Figure 1); the basin narrows offshore Ibaraki around sites BS101 and BS102 (Figure 1).

A flat submarine terrace called the mid-slope terrace (MST), which is over 150-km wide, strikes in parallel to the trench axis at depths of approximately 4,000 to 5,500 m offshore Sanriku. Surface erosive failure makes the slope between the MST and the trench axis steep. Within the outer wedge beneath the middle slope, a clear reflector exists on the seismic profile that is due to the velocity contrast between the trenchward side and landward side of the wedge (Figure 2). The velocity of the former is approximately 1.7 to 3.4 km/s, and the velocity of the latter is approximately 4.2 km/s (Tsuru et al. 2002). This boundary is a back-stop interface.

To the south offshore of Fukushima, the lowest frontal slope near the trench is divided into two slopes that are gentler compared to those offshore of Sanriku. The outer rise of the Pacific Plate is well developed around the Kuril Trench, but it is poorly developed in the south offshore of Fukushima. A thick sedimentary wedge with low-P-wave velocity is present near the foot of the landward slope (Ludwig et al. 1966).

The Daiichi Kashima seamount and Katori seamount on the Pacific Plate are colliding with the trench axis off the coast of Ibaraki at the southern part of the Japan Trench. The Daiichi Kashima seamount is split into two bodies with a normal fault (Lallemand et al. 1989; von Huene and Lallemand 1990). von Huene and Lallemand (1990) proposed a deformation process of erosive topography due to the horst-graben structure collision in the Japan Trench, which involves forearc deformation and healing of the landward slopes, thus resulting in tectonic erosion.

The geodetic leveling in Japan over the past, approximately 70 years, indicates that the coast of the southern part of northeastern Japan is topographically stable. However, a large depression has been recognized in the

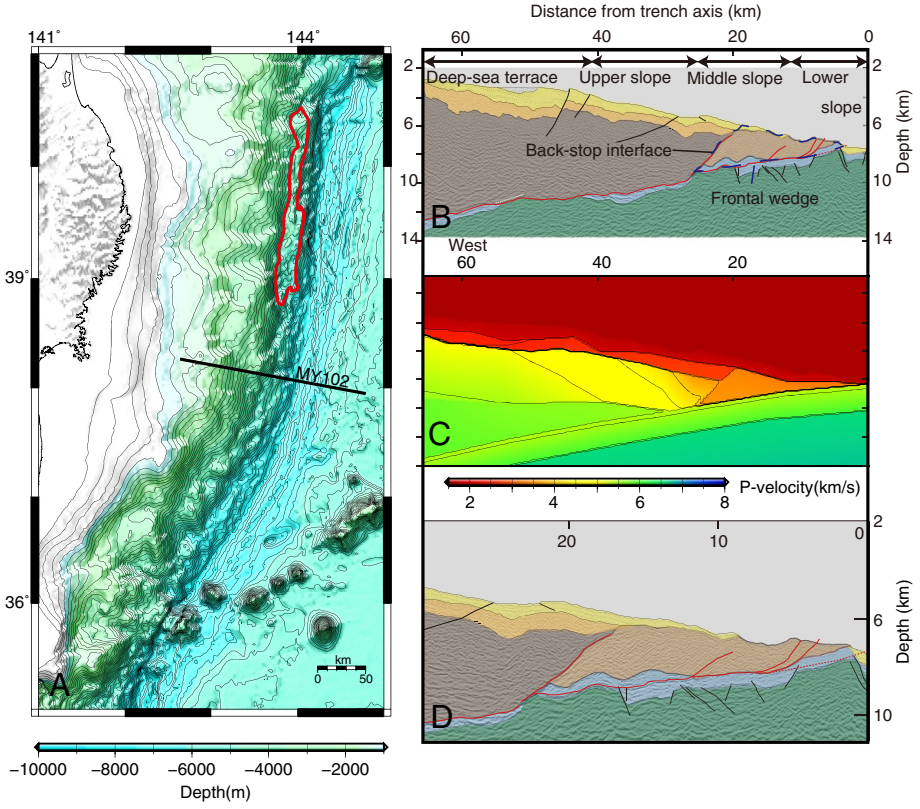

Figure 2 Seafloor topography of the forearc off northeastern Japan. (A) The red circled area represents the mid-slope terrace. **(B)** Cross section of the forearc wedge in the Japan Trench (modified from Kimura et al. 2012). The slope surface is separated into four slopes by the tilt angle: the deep-sea terrace, the upper slope, the middle slope, and the lower slope. The area surrounded by the blue dotted line is the frontal wedge. **(C)** The profile of MY102 drawn by seismic refraction data. Within the outer wedge beneath the middle slope, a clear reflector exists on the seismic profile that is due to the velocity contrast between the trenchward side and landward side of the wedge. This reflector is named the back-stop interface (Tsuru et al. 2002). **(D)** Enlarged figure of the frontal wedge whose geometry is analyzed in this research.

northern part of Tohoku and it is characterized by steep slopes that are distributed from the land to the Pacific Ocean (Dambara 1971; El-Fiky and Kato 1999; Matsu'ura et al. 2009). Ikeda (2003) and Matsu'ura et al. (2009) pointed out that the coastline facing the Pacific Ocean in northeast Japan has been uplifting by 0.1 to 0.2 mm/year based on the old shoreline of the last interglacial period (100 to 125 kyr). It should also be noted that the scale contradiction might be due to deformation.

The upper plate of the northeast Japan forearc consists mainly of Cretaceous to Neogene strata and igneous rock. The incoming sediment on the Pacific Plate is composed of a Cretaceous sequence of cherts and a thick pile of Neogene siliceous clay and hemi-pelagic clay (The Shipboard Scientific Party 1980; Chester et al. 2013). The landward lower slope around the trench axis, on which we focus in this paper, is composed of pelagic/hemi-pelagic sediment (Mann and Müller 1980).

The 2011 Tohoku-Oki earthquake (Mw 9.0) propagated a fault rupture extending to the Japan Trench, which generated a large tsunami by seafloor displacement (e.g., Fujii et al. 2011; Ide et al. 2011). Based on differences in the bathymetry detected from seismic profiles before and after the earthquake, the seafloor of the outermost landward slope has been demonstrated to have moved approximately 50 m as a large slump toward the trench and it has been uplifted by approximately 7 to 10 m (Fujiwara et al. 2011; Kodaira et al. 2012). In addition, changes in the internal structure of the outer wedge also indicate that the fault rupture reached the trench axis (Tsuji et al. 2013). Kimura et al. (2012) analyzed a cross section of the Japan Trench using the critical taper theory (Davis et al. 1983), and they estimated the effective frictional coefficient of the plate boundary megathrust. Sampled cores and profiles taken after the earthquake indicate that the frontal deformation is characterized by rotational slumping extending to the trench axis (Strasser et al. 2013).

Data and methods

We focused on the frontal wedge of the Japan Trench and used 12 profiles of seismic reflection and refraction survey data at the frontal wedges of the Japan Trench to analyze the topographical parameters and obtain the frictional properties (Figure 1). We focused on these areas because the sediments of the frontal wedge are composed only of low-P-wave velocity material (Tsuru et al. 2002). This enables us to assume a wedge of uniform velocity and obtain approximate depth-converted data from time sections.

In applying the theory of a critically tapered Coulomb wedge (Davis et al. 1983) to calculate frictional properties of the décollement, it is necessary to obtain the topographic parameters of the surface slope angle and the décollement dip angle from depth seismic profiles.

Data acquisition

We obtained two parameters representing the wedge configuration, i.e., the taper angle α + β (where α is the surface slope angle and β is the décollement dip angle) and the angle between the décollement and the back-stop interface (ω), from the sea-beam topographic map and seismic reflection profiles (Tsuru et al. 2002; Tsuji et al. 2011) (Figures 1 and 3). The original seismic reflection data represent only a section of time, and it is difficult to estimate the dip angles β and ω accurately because errors increase significantly when converting the times to depths by assuming the velocity. Generally, it is better to use the results of both reflection data and those obtained by the refraction method to estimate the depth.

In this study, we used the results reported by Tsuru et al. (2002), Tsuji et al. (2011), and the JAMSTEC (Japan

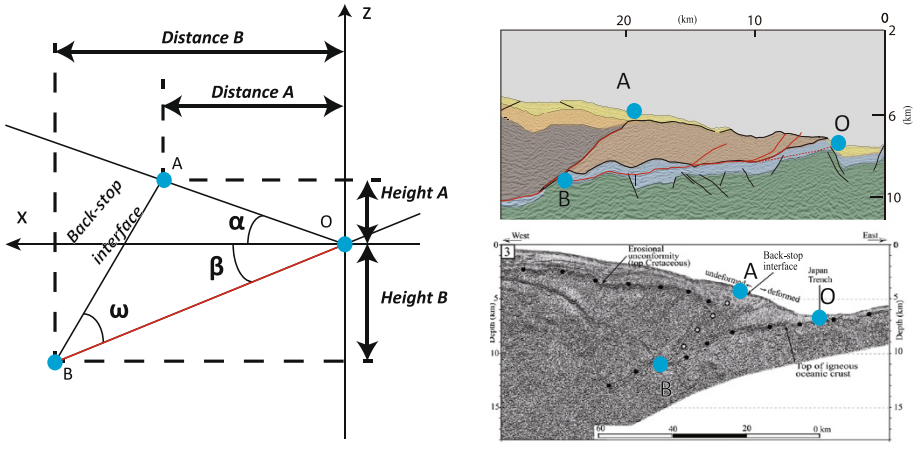

Figure 3 Schematic of the geometry of the wedge-shaped deformed zone (modified from Tsuru et al. 2002). α: the slope angle of the sea-bottom surface. β: the décollement dip angle. ω: the angle between the décollement and back-stop interface. The red line on the bottom represents the décollement or plate boundary for which we obtained the effective coefficient of basal friction by the critical taper theory.

Agency for Marine-Earth Science and Technology) crustal structural database site (https://www.jamstec.go.jp/jamstec-e/IFREE_center/index-e.html). Tsuru et al. (2002) presented seismic profiles (HK203, AM101, AM102, SR101, MY101, MY104, FK101, FK102, and BS102), whereas Tsuji et al. (2011) presented the depth-converted profile of MY102. We used the migrated seismic profiles of MY103 and BS101 from the JAMSTEC crustal structural database site. According to Tsuru et al. (2002), the frontal wedge is a low velocity structure of approximately 1.7 to 3.4 km/s. By applying a velocity of approximately 1.7 km/s to the most frontal part, we were able to convert the travel times to depths.

Considering the *x*-*z* coordinate with an origin at the Japan Trench axis as shown in Figure 3, we can define the point of intersection of the plate boundary décollement and the back-stop interface, which might be a splay fault, and also the point of intersection of the slope surface and the back-stop interface.

The depth sections of HK203, AM101, AM102, SR101, MY101, MY104, FK101, FK102, and BS102 used in this study were converted by the pre-stack depth migration (PSDM) velocity analysis by Tsuru et al. (2002), but the sections of MY102 were converted by the stacking velocity analysis by Tsuji et al. (2011). The difference in the conversion methods may have affected the converted depths and the values of the taper angles. Specifically, since errors in stacking velocity analyses (Tsuji et al. 2011) can be larger than those in PSDM analyses (Tsuru et al. 2002), the taper angles along the seismic lines of MY102 may have larger errors compared to those on the other lines.

Because of the difficulty in determining accurate seismic velocities for the deeper lithologies, information on the location of the décollement and back-stop interface is limited along seismic lines MY103 and BS101.

In the wedge near point B in Figure 3, Tsuru et al. (2002) located a lithologic layer characterized by a P-wave velocity of approximately 3.4 km/s. The thickness of this layer is approximately 0.3 s, and the décollement dip angle β was calculated to be larger by approximately 0.87 when compared to the values under the velocity of approximately 1.7 km/s. Accordingly, we set a ±1° error range for the angle estimates of the three types of angle (i.e., α, β, and ω), thus accounting for the inferred error in velocity for the sedimentary wedge (Tsuru et al. 2002). The wavelength of the reflector of the décollement is approximately 200 m (e.g., Tsuru et al. 2002), and the angle error produced by the wavelength was calculated to be approximately 0.57°, which is within the error range of ±1°.

The maximum slip area of the 2011 Tohoku-Oki earthquake is located along MY102. It is notable that all of the data in this study were acquired before the 2011 Tohoku-Oki earthquake. The last large earthquake before the 2011 Tohoku-Oki earthquake was the Mw 8.1 event in 1933, which might have affected the prism to become a steady-state and formed interseismic geometry (e.g., Fagereng 2011; Tajima et al. 2013).

Methods

In the present study, we obtained the slope angle of the sea-bottom surface (α), the décollement dip angle β, and the angle between the décollement and back-stop interface ω from the 12 profiles of seismic reflection and refraction survey data taken at the frontal wedges of the Japan Trench (Figures 1 and 3). As shown in Figure 3, by assuming three points, namely, the trench axis at the deepest location (O), the intersection of the surface slope and the back-stop interface (A), and the intersection of the décollement and the back-stop interface (B) (Figure 3), we could define the slope angle α [= atan (Height A/Distance A)] and the décollement dip angle β [= atan (Height B/Distance B)]. The back-stop interface was referred from the figures by Tsuru et al. (2002) and Tsuji et al. (2011). Since the back-stop interface was not observed at BS102 and BS103, we tentatively set A and B at the horizontal distance of 20 km from the trench axis to obtain α and β from these profiles.

The critical taper theory, first introduced by Davis et al. (1983) and Dahlen (1984), is a mechanical model based on Mohr's circle and Coulomb failure criteria that has been applied to subduction zones in various studies to describe the mechanics and physical properties of wedges (e.g., Wang et al. 2010; Fagereng 2011; Kimura et al. 2012; Cubas et al. 2013). According to this theory, by assuming that (1) the tip of the wedge is tapered, (2) the sediments added to the prism are non-viscous, and (3) the internal stress is always at the critical state just before failure, the taper angle (α + β) of the wedge is controlled by the relative strengths of the wedge material and basal fault, i.e., the coefficient of internal friction averaged over the wedge (μ), the pore fluid pressure ratio within the wedge (λ), and the effective coefficient of basal friction $\left(\mu_b'\right)$.

To calculate the effective coefficient of basal friction and pore fluid pressure ratio, we used the theory and formulas by Dahlen (1984), Adam and Reuther (2000), and Wang et al. (2010). We obtained the parameters by drawing cross plots between the λ and effective coefficient of basal friction $\left(\mu_b'\right)$ (Figure 4) by referring to Wang et al. (2010). The equations used to obtain μ_b' and to draw the limb of the cross plot (Figure 4) to constrain λ are explained below. As stated earlier, the following equations correspond respectively to Eqs. (10), (9), (17), and (18) of Dahlen (1984).

The slope angle α modified in subaerial conditions is formulated as

$$\alpha' = \tan^{-1}\left[\left(\frac{1-\rho_w/\rho}{1-\lambda}\right)\tan\ \alpha\right]$$

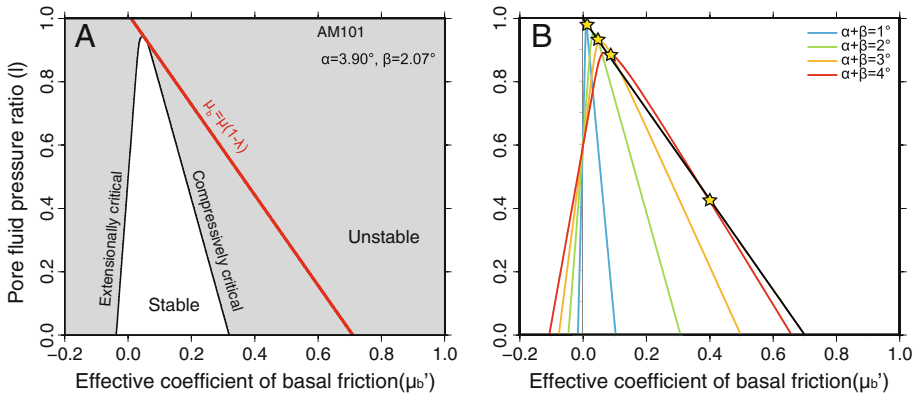

Figure 4 Cross plots between the λ and effective coefficient of basal friction. (A) Calculated critical values of the Hubbert-Rubey pore fluid pressure ratio (λ) and basal friction (μ_b') of the wedge. Extensionally critical states form on the left limb of the critical-state curve, whereas compressively critical states form on the right limb. The white area below the curve represents the stable region. The straight-line tangent to critical-state curve represents the condition of $\mu_b' = \mu(1-\lambda)$, where α is the surface slope angle and β is the décollement dip angle. **(B)** Parameter sensitivity of the taper angle; data were modified and applied to survey sites AM101 and SR101 (from Wang et al. 2010). Calculations were performed assuming ρ = 2,700 kg/m^3, ρw = 1,000 kg/m^3.

where ρ is the wedge sediments density, ρw is the fluid density, and λ is the Hubbert-Rubey pore fluid pressure ratio. It should be noted that if the wedge is in a dry condition (ρ_w = 0, λ = 0), the following approximation can be applied: $\alpha' = \alpha$. Then, the uniform angle between the most compressive principal stress σ_1 and the upper surface ψ_0 can be formulated as

$$\psi_0 = \frac{1}{2}\tan^{-1}\left(\frac{\sin\alpha'}{\sin\phi}\right)\tan\ \alpha$$

where ϕ is the angle of internal friction averaged over the wedge and ψ_0 is the angle between σ_1 and the upper slope. Under a non-cohesive condition, this equation would be valid for the entire wedge except at the boundary along the basement (e.g., Dahlen 1984).

Since along-strike stresses are not regarded in the critical taper model, the following simple geometric formula and key equation of the critical taper model can be applied:

$$\alpha + \beta = \psi_b - \psi_0$$

where ψ_b is the angle between σ_1 and the basal surface. Then, the effective coefficient of basal friction (μ_b') is obtained from the Mohr-Coulomb criterion and stress balance of the basal condition:

$$\mu_b' = \frac{\tan 2\psi_b}{\csc\phi\sec\psi_b - 1}$$

To draw the limb of the cross plot between μ_b' and λ, we set λ as a parameter ranging between 0 and 1.

We obtained the pore fluid pressure ratio λ from the intersection between the limb and the straight line defined as

$$\mu_b' = \mu(1-\lambda)$$

This equation assumes the condition that the basal fault is relatively strong and that the wedge is in a compressively critical state (Wang et al. 2010). This can be applied to the Japan Trench since this area is thought to be an erosional margin (von Huene and Lallemand 1990). Given the geometry and strength, the wedge is characterized by an extensionally critical state if the basal friction is sufficiently low, whereas under high basal friction, a compressively critical state is dominant (e.g., Wang and Hu 2006). In the calculations, we assumed μ to be 0.7 (ϕ = 35°) by referring to Wang et al. (2010) and ρ and ρw to be 2,700 and 1,000 kg/m^3, respectively, by referring to Kimura et al. (2012). It should be noted that most of the prior studies that used this theory applied a small angle of approximation such as sinα = α, and because of this, the calculations can have accuracies below 95% for angles above 30°.

Results

The obtained taper angle (α + β) and the angle between the décollement and back-stop interface ω are shown in Figure 5A,B respectively, along with the latitudes of the locations in the seismic profiles. Results for the calculated effective coefficient of basal friction and the Hubbert-Rubey pore fluid pressure ratio, which was derived using the critical taper theory from the same location, are presented in Figure 5C,D respectively. All of the plots in Figure 5A,B,C,D represent the data before the 2011 earthquake. The taper angles of FK102, MY102, and SR101 are approximately 5° larger than the average of the studied areas (approximately 7.07°) (Figures 3 and 5A).

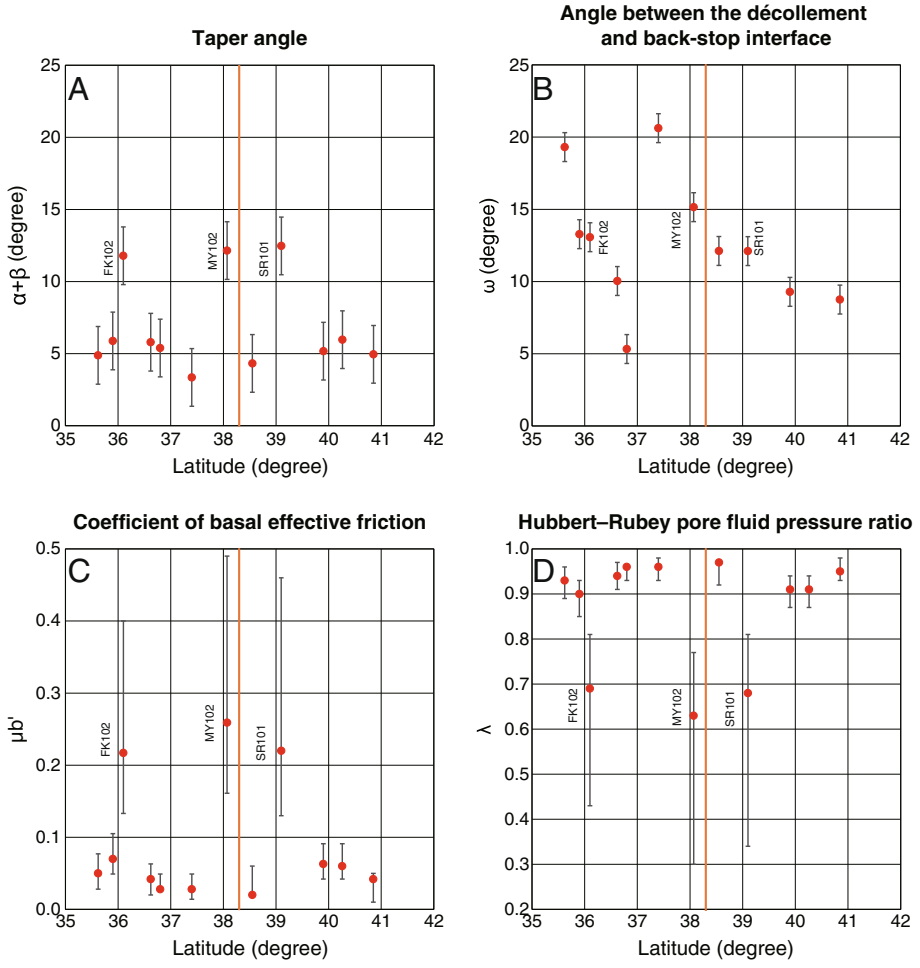

Figure 5 The topographic parameters obtained from the seismic cross sections. The results analyzed from critical taper theory. Orange line: the latitude of the epicenter of the 2011 Tohoku-Oki earthquake. **(A)** North-south variation of the taper angle (α + β). **(B)** North-south variation of the angle between the décollement and back-stop interface. **(C)** North-south variation of the effective coefficient of basal friction. **(D)** North-south variation of the Hubbert-Rubey pore fluid pressure ratio.

The angle between the décollement and the back-stop interface ω tends to decrease toward the north, except at FK101 and MY102 (Figure 5B). The effective coefficients of basal friction μ_b' at FK102, MY102, and SR101 are larger and have a wider range compared to the other areas (Figure 5C). The average of the pore fluid pressure ratio λ is approximately 0.91, which is relatively high. However, the λ values at profiles FK102, MY102, and SR101 were smaller than this average.

A positive correlation exists between the taper angles and μ_b', and a negative correlation was observed between the taper angles and λ. The areas near the Daiichi Kashima seamount at a latitude of approximately 36° have large taper angles, and therefore the μ_b' is relatively high (approximately 0.22) and the λ is low (approximately 0.69) in this region. It should be noted that the range of μ_b' values in this area is wider than the range in the other areas. The profile of MY102 crossing the maximum slip area of the 2011 Tohoku-Oki earthquake presents a relatively large taper angle with high μ_b' (approximately 0.26) and low λ (approximately 0.63) values. SR101 (Figure 5A) also presents a large taper angle with higher μ_b' (approximately 0.22) and lower λ (approximately 0.68) values relative to the average values of the studied areas $\left(\mu_b' = 0.09, \lambda = 0.87\right)$.

Discussion

According to interpretations of the seismic profile, the frontal wedge (approximately 20 km from the trench axis) was in a state of compression before the 2011 earthquake (Tsuru et al. 2002; Kimura et al. 2012). In the present study, we calculated the effective coefficient of basal friction by applying the critical taper theory under the compressive condition.

The relationship between the effective coefficient of basal friction and the pore fluid pressure ratio is presented in Figure 4, and it was derived on the basis of the equations by Wang et al. (2010). The compressively critical state appears on the right limb of the red line and the extensionally critical state forms on the left limb of the line (Figure 4). In Figure 4A, the curved line dividing stable and unstable regions represents the function of μ_b', which depends on the pore fluid pressure ratio λ at the critical state. The straight line is formulated as $\mu_b' = \mu(1-\lambda)$, where μ is the coefficient of internal friction averaged over the wedge defined as $\mu = \tan\phi$ and ϕ is the angle of internal friction averaged over the wedge.

In the present study, we assumed ϕ to be 35°, which is an average value commonly recognized in soil and rock mechanics; therefore, the internal friction averaged over the wedge μ is approximately 0.70. The contact point of the two lines presents the effective coefficient of basal friction and pore fluid pressure at the point where the wedge reaches a compressively critical state under the constant coefficient of internal friction averaged over the wedge μ. The sensitivity of μ_b' to the taper angle is shown in Figure 4B.

The results of the calculated effective coefficient of basal friction μ_b' were variable among the 12 survey lines (Figure 5). At three locations, large taper angles imply low pore fluid pressure ratios within the wedge and relatively large values of μ_b'. These relationships are based on the intrinsic nature of the critical taper theory because the taper angle and basal frictional coefficient have a positive correlation, whereas the pore pressure ratio and taper angle have a negative correlation. Strong basal friction is indicated by the large taper angle, which may appear in the topography if the dip angle of the oceanic plate is constant (Davis et al. 1983; Dahlen 1984).

In addition, μ_b' and λ show large error bars at three profiles (FK102, MY102, and SR101) (Figure 5C,D). In Figure 4B, the intersection of the critical-state curve and $\mu_b' = \mu(1-\lambda)$ (represented by the star marks) moves with a change in the taper angle. The taper angle becomes larger in the order from blue, green, yellow to red in Figure 4B. This means that as the taper angle becomes larger, the effective coefficient of friction at the critical state increases to a wider range along with a decrease in the pore fluid pressure ratio. This is the reason for the large error bars of μ_b' and λ in Figure 5C,D.

Taking this calculation output into account, we next discuss the values for each of these three areas: FK102, MY102, and SR101. In the southernmost area, FK102 is considered to have been influenced by the collisions of the Katori seamount and the Daiichi Kashima seamount as described by Lallemand and Xavier (1987) and Lallemand et al. (1989). Lallemand et al. (1994) applied the critical taper theory to this area and suggested that the wedge gains a larger taper angle under the critical state because of the initial stage of seamount subduction. In addition to the changes in geometry caused by seamount subduction, Fagereng (2011) suggested that the fracturing increases around the seamounts, which may affect the permeability and possibly reduce the pore pressure. Moreover, Scholz and Small (1997) suggested that the subducting seamount increases the stress normal to the fault because of the flexural rigidity of the upper plate, and as a result this makes the shear strength greater. Therefore, the effective frictional coefficient might become high with an increase in the taper angle of the wedge due to the seamount collision. Along seismic line BS101, the slope angle α and décollement dip angle β are relatively large, and the latter increases toward the west thereby causing the décollement to shallow out in the landward direction as indicated by the migrated profile of BS101 (https://www.jamstec.go.jp/jamstec-j/IFREE_center/data/cruise_data/KR01-10section.html#bs101). This is also likely caused by the subduction of seamounts.

The northern areas of MY102 and SR101 have large taper angles even though these areas are not characterized by seamount collisions. Sasaki and Tamaki (2005) reported that the area over SR101 and MY102 is a topographically transitional area that separates the southern region from the northern region of the Japan Trench; the MST generally exists only in the northern part of the Japan Trench (Figure 1) starting between SR101 and MY102, and it is not observed in the south.

In addition to this topographic characteristic, Fujie et al. (2002) reported that a seismic gap can be recognized in the landward area between SR101 and MY102. Additionally, well-developed horst-graben structures have been reported in this area (Honza 1977; Tanioka et al. 1997). Thus, the area of the 2011 earthquake rupture was topographically and seismically unique from other forearc regions in the Japan Trench.

The north and south ends of the coseismic slip area of the 2011 earthquake (Figure 1) compiled by Chester et al. (2013) are in almost complete agreement with the locations of SR101 and FK102, respectively. This coincidence suggests that strain energy accumulation near the trench axis around MY102 occurred because of the relatively high friction and later caused a large slip and collapse of the wedge. The basal décollement around SR101 also has a large effective coefficient of basal friction, but the fault rupture during the 2011 earthquake did not reach this area and did not overcome the frictional strength at SR101, even though the rupture propagated to the south and to the north at the shallow plate boundary. The reason for this is unclear at the present time.

Cubas et al. (2013) reported that the prism became extensionally critical after the Tohoku-Oki earthquake in association with the occurrence of normal faults and the increase in the pore fluid pressure ratio; thus, this infers that the fault is weak $\left(\mu_b^{'} = 0.14 + 0.14/-0.04\right)$. Ujiie et al. (2013) also found that the fault is frictionally weak. Therefore, there is an apparent contradiction between their results and our results that show a strong patch in the maximum slip area of the 2011 Tohoku-Oki earthquake. In our results, the $\mu_b^{'}$ of MY102 is 0.26 + 0.23/−0.10. We propose that the 2011 Tohoku-Oki earthquake rupture may have propagated to a location with a relatively high effective coefficient of basal friction, but that dynamic weakening due to factors such as thermal pressurization must have been significant (e.g., Ujiie et al. 2013), thus leading to very low coseismic friction and the change from a compressive to an extensional critical wedge.

Conclusions

We applied the critically tapered Coulomb wedge theory to the topography and seismic reflection data of 12 sites across the toe of the forearc wedge in the Japan Trench, and we observed north-south variation in the effective coefficient of basal friction. The effective friction coefficient was remarkably large at three locations, which led us to the following conclusions.

(1) The southernmost area is characterized by a large taper angle, which suggests that there is a high effective coefficient of basal friction if the prism is in a steady state. This area coincides with the location where a seamount is colliding offshore of Fukushima.
(2) The second area with a high effective coefficient of basal friction coincides with the maximum slip location during the 2011 Tohoku-Oki earthquake. The area of the 2011 earthquake rupture was topographically unique from other forearc regions in the Japan Trench before the earthquake. The strain energy accumulation near the trench axis around MY102 may have proceeded because of the relatively high friction prior to the event. Later, dynamic weakening must have been significant leading to the very low coseismic friction and change from a compressional to an extensional critical wedge, which caused the large slip and collapse of the wedge.
(3) The third location with a high effective coefficient of basal friction is the site offshore of Sanriku, where there are neither seamount collisions nor rupture propagation. These characteristics may account for the well-developed horst-graben structures of this area.

The characteristics of the taper angle, effective coefficient of basal friction, and pore fluid pressure ratio along the Japan Trench presented in this study may contribute to the understanding of the relationship between the long-term, steady-state geometry of the prism and the potential for the generation of seismo-tsunamigenic slips.

Abbreviation

MST: Mid-slope terrace.

Competing interests

The authors declare that they have no competing interests.

Authors' contributions

TF, SK and TS participated in the discussion based on the data of important previous studies. JK, YK, MH, RF, AY, YH, JA, and GK participated in the discussion of research and give a lot of comments and suggestion.
All authors read and approved the final manuscript.

Acknowledgements

This work was supported by a Ministry of Education, Culture, Sports, Science, and Technology (MEXT) Science Research Grant (No. 21107005) and a Japan Society for the Promotion of Science (JSPS) Grant (No. 23244099, research A).

Author details

[1]Department of Earth and Planetary Science, The University of Tokyo, Tokyo 113-0033, Japan. [2]Japan Agency for Marine-Earth Science and Technology (JAMSTEC), 2-15 Natsushima-cho, Yokosuka, Kanagawa 237-0061, Japan. [3]Ocean Engineering and Development Corporation (OED), 3-2 Kobuna-cho, Nihombashi, Chuo-ku, Tokyo 103-0024, Japan. [4]Department of Natural History Sciences, Graduate School of Science, Hokkaido University, N10 W8, Sapporo 060-0810, Japan. [5]Department of Earth and Environmental Sciences, Graduate School of Science and Engineering, Kagoshima University, 1-21-35 Korimoto, Kagoshima 890-0065, Japan. [6]Atmosphere and Ocean Research Institute, The University of Tokyo, 5-1-5 Kashiwanoha, Kashiwa-shi, Chiba 277-8564, Japan.

Received: 9 March 2014 Accepted: 5 November 2014
Published online: 19 November 2014

References

Adam J, Reuther CD (2000) Crustal dynamics and active fault mechanics during subduction erosion. Application of frictional wedge analysis on to the North Chilean Forearc. Tectonophysics 321:297–325
Chester FM, Rowe C, Ujiie K, Kirkpatrick J, Regalla C, Remitti F, Toczko S (2013) Structure and composition of the plate-boundary slip zone for the 2011 Tohoku-Oki earthquake. Science 342:1208–1211
Cubas N, Avouac JP, Leroy YM, Pons A (2013) Low friction along the high slip patch of the 2011 Mw 9.0 Tohoku-Oki earthquake required from the wedge structure and extensional splay faults. Geophys Res Lett 40(16):4231–4237
Dahlen FA (1984) Noncohesive critical Coulomb wedges: an exact solution. J Geophysical Res 89(B12):10125–10133
Dambara T (1971) Synthetic vertical movements in Japan during the recent 70 years. J Geodetic Soc Japan 17(3):100–108
Davis D, John S, Dahlen FA (1983) Mechanics of fold-and-thrust belts and accretionary wedges. J Geophysical Res 88(B2):1153–1172
DeMets C, Gordon RG, Argus DF, Stein S (1994) Effect of recent revisions to the geomagnetic reversal time scale on estimates of current plate motions. Geophys Res Lett 21(20):2191–2194
Dietz RS (1954) Marine geology of northwestern Pacific: description of Japanese bathymetric chart 6901. Geol Soc Am Bull 65(12):1199–1224
El-Fiky GS, Kato T (1999) Interplate coupling in the Tohoku district, Japan, deduced from geodetic data inversion. J Geophysical Res 104(B9):20361–20377
Fagereng Å (2011) Wedge geometry, mechanical strength, and interseismic coupling of the Hikurangi subduction thrust, New Zealand. Tectonophysics 507(1):26–30
Fujie G, Kasahara J, Hino R, Sato T, Shinohara M, Suyehiro K (2002) A significant relation between seismic activities and reflection intensities in the Japan Trench region. Geophys Res Lett 29(7):4-1–4-4

Fujie G, Miura S, Kodaira S, Kaneda Y, Shinohara M, Mochizuki K, Uehira K (2013) Along-trench structural variation and seismic coupling in the northern Japan subduction zone. Earth Planets Space 65:75–83

Fujii Y, Satake K, Sakai SI, Shinohara M, Kanazawa T (2011) Tsunami source of the 2011 off the Pacific coast of Tohoku earthquake. Earth Planets Space 63(7):815–820

Fujiwara T, Kodaira S, No T, Kaiho Y, Takahashi N, Kaneda Y (2011) The 2011 Tohoku-Oki earthquake: displacement reaching the trench axis. Science 334(6060):1240–1240

Honza E (1977) Geological investigation of Japan and southern Kurile Trench and slope areas: GH 76–2 cruise, April–June 1976. Geological Survey of Japan 7. https://www.gsj.jp/publications/pub/cruise-rep/. doi:10.2973/dsdp.proc.5657.108.1980

Ide S, Baltay A, Beroza GC (2011) Shallow dynamic overshoot and energetic deep rupture in the 2011 Mw 9.0 Tohoku-Oki earthquake. Science 332(6036):1426–1429

Ikeda Y (2003) Contradiction of geodetic strain rate and geological strain rate. Chikyu Mon 25(2):125–129

Kimura G, Hina S, Hamada Y, Kameda J, Tsuji T, Kinoshita M, Yamaguchi A (2012) Runaway slip to the trench due to rupture of highly pressurized megathrust beneath the middle trench slope: the tsunamigenesis of the 2011 Tohoku earthquake off the east coast of Northern Japan. Earth Planet Sci Lett 339:32–45

Kodaira S, No T, Nakamura Y, Fujiwara T, Kaiho Y, Miura S, Taira A (2012) Coseismic fault rupture at the trench axis during the 2011 Tohoku-oki earthquake. Nat Geosci 5(9):646–650

Lallemand S, Xavier LP (1987) Coulomb wedge model applied to the subduction of seamounts in the Japan Trench. Geology 15(11):1065–1069

Lallemand S, Ray C, von Huene R (1989) Subduction of the Daiichi Kashima seamount in the Japan Trench. Tectonophysics 160(1):231–247

Lallemand S, Philippe S, Jacques M (1994) Coulomb theory applied to accretionary and nonaccretionary wedges: possible causes for tectonic erosion and/or frontal accretion. J Geophysical Res 99(B6):12033–12055

Ludwig WJ, Ewing JI, Ewing M, Murauchi S, Den N, Asano S, Noguchi I (1966) Sediments and structure of the Japan Trench. J Geophys Res 71(8):2121–2137

Mann U, Müller G (1980) Composition of sediments of the Japan Trench transect, legs 56 and 57, Deep Sea Drilling Project. DSDP volume LVI and LVII table of contents., doi:10.2973/dsdp.proc.5657.133.1980

Matsu'ura T, Furusawa A, Saomoto H (2009) Long-term and short-term vertical velocity profiles across the forearc in the NE Japan subduction zone. Quat Res 71(2):227–238

Nakanishi M, Tamaki K, Kobayashi K (1989) Mesozoic magnetic anomaly lineations and seafloor spreading history of the northwestern Pacific. J Geophysical Res 94(B11):15437–15462

Sasaki T, Tamaki K (2005) Seafloor morphology of the frontal part of the trench landward slope in the Japan Trench and proceedings of the subduction erosion off Miyagi. Earth Mon 51:125–129

Scholz CH, Small C (1997) The effect of seamount subduction on seismic coupling. Geology 25(6):487–490

Strasser M, Kölling M, dos Santos FC, Fink HG, Fujiwara T, Henkel S, Wefer G (2013) A slump in the trench: tracking the impact of the 2011 Tohoku-Oki earthquake. Geology 41(8):935–938

Tajima F, Mori JJ, Kennett BL (2013) A review of the 2011 Tohoku-Oki earthquake (Mw 9.0): large-scale rupture across heterogeneous plate coupling. Tectonophysics 586:15–34

Tanioka Y, Ruff L, Satake K (1997) What controls the lateral variation of large earthquake occurrence along the Japan Trench? Island Arc 6(3):261–266

The Shipboard Scientific Party (1980) Site 436. Japan Trench outer rise. Leg 56. DSDP volume LVI and LVII table of contents., doi:10.2973/dsdp.proc.5657.107.198

Tominaga M, Sager WW, Tivey MA, Lee SM (2008) Deep-tow magnetic anomaly study of the Pacific Jurassic Quiet Zone and implications for the geomagnetic polarity reversal timescale and geomagnetic field behavior. J Geophys Res 113(B7), B07110

Tsuji T, Ito Y, Kido M, Osada Y, Fujimoto H, Ashi J, Matsuoka T (2011) Potential tsunamigenic faults of the 2011 off the Pacific coast of Tohoku earthquake. Earth Planets Space 63(7):831–834

Tsuji T, Kawamura K, Kanamatsu T, Kasaya T, Fujikura K, Ito Y, Kinoshita M (2013) Extension of continental crust by anelastic deformation during the 2011 Tohoku-oki earthquake: the role of extensional faulting in the generation of a great tsunami. Earth Planet Sci Lett 364:44–58

Tsuru T, Park JO, Miura S, Kodaira S, Kido Y, Hayashi T (2002) Along-arc structural variation of the plate boundary at the Japan Trench margin: implication of interplate coupling. J Geophys Res 107(B12):2357

Ujiie K, Tanaka H, Saito T, Tsutsumi A, Mori JJ, Kameda J, Toczko S (2013) Low coseismic shear stress on the Tohoku-Oki megathrust determined from laboratory experiments. Science 342(6163):1211–1214

von Huene R, Lallemand S (1990) Tectonic erosion along the Japan and Peru convergent margins. Geol Soc Am Bull 102(6):704–720

Wang K, Hu Y (2006) Accretionary prisms in subduction earthquake cycles: the theory of dynamic Coulomb wedge. J Geophysical Res 111(B6), B06410

Wang K, Hu Y, von Huene R, Kukowski N (2010) Interplate earthquakes as a driver of shallow subduction erosion. Geology 38(5):431–434

doi:10.1186/s40623-014-0153-3
Cite this article as: Koge *et al.*: **Friction properties of the plate boundary megathrust beneath the frontal wedge near the Japan Trench: an inference from topographic variation.** *Earth, Planets and Space* 2014 **66**:153.